Journal of Alloys and Compounds 509 (2011) 2081–2086

Contents lists available at ScienceDirect

Journal of Alloys and Compounds

journal homepage: www.elsevier.com/locate/jallcom

High cycle fatigue property of Ti-600 alloy at ambient temperature

Zeng Liying[a,b,*], Zhao Yongqing[b], Hong Quan[b], Yang Guanjun[a]

[a] School of Metallurgical Engineering, Xi'an University of Architecture and Technology, Xi'an 710055, PR China
[b] Northwest Institute for Nonferrous Metal Research, Xi'an 710016, PR China

ARTICLE INFO

Article history:
Received 7 September 2010
Received in revised form 10 October 2010
Accepted 28 October 2010
Available online 4 November 2010

Keywords:
High temperature Ti alloys
Ti-600 alloy
Fatigue strength
Rare earth phases

ABSTRACT

Smooth axial fatigue tests were carried out at ambient temperature on one kind of near alpha titanium alloy named after Ti-600 at a frequency of 120–130 Hz and with two kinds of load ratios. The high cycle fatigue (HCF) strength for the solutioned and aged alloy is found to be 475 MPa fatigued with a load ratio R of 0.1, and which is 315 MPa with a load ratio R of −1. The observed high HCF strength for the samples fatigued with a load ratio R of 0.1 is attributed to its overlapping fine and thin plate like α + β phase microstructure. During the crack propagation region, at the same stress of 600 MPa, the sample with a fatigue life of 1.78×10^6 cycles has a better fatigue resistance than that of the sample with a fatigue life of 8.61×10^5 cycles, because of its smaller striation distance, its well-developed secondary cracks, more wider and coarsened α lathes precipitated at grain boundaries, and the heavily arranged interlacing transformed β microsructures. The average grain size of rare earth phases varies from several micrometers to 0.2 μm, no cracks corresponding to rare earth particles can be initiated.

1. Introduction

Titanium and titanium alloys have found many applications in aerospace, marine, chemical, sporting goods, power generation and biomedical industries. When considering the phase equilibrium and microstructure stability, the use of conventional titanium alloys have restricted to below 600 °C because of alpha-case formation originated from oxygen absorption, which has been shown to severely limit the high-temperature capability of alloys in terms of mechanical properties. However, owing to the requirements for advanced aerospace industry for increased performances and higher using temperatures, more and more attention has been paid on titanium alloys which can be used at 600 °C or even higher temperature for a long time [1–3]. Several near α titanium alloys have been developed in order to meet above demands [4–6]. Ti-600, developed by Northwest Institute for Nonferrous Metal Research (NIN) in China, is a near alpha titanium alloy designed for applications up to 600 °C [7–9].

In materials science, fatigue is the progressive and localized structural damage that occurs when a material is subjected to cyclic loading. The maximum stress values are less than the ultimate tensile stress limit, and may be below the yield stress limit of the material. 80% of service failure is attributed to fatigue [10]. A detailed study of the cyclic fatigue response of the chosen titanium alloy is important for its selection and eventual use in a spectrum of performance-critical industries spanning aerospace, automotive, marine and even commercial products.

Because Ti-600 alloy components in turbine engines work in high cycle loading condition, fatigue failure becomes the main invalidation mode for the components, so, it has the obvious engineering value to investigate the fatigue behavior of the alloy. As a new generation high temperature Ti alloy, mechanical behavior of the alloy at ambient temperature and its service temperature has widely been investigated by several researchers [7,8]. In the recent years, with the understanding of the microstructure characteristic and mechanics properties of the alloy, the application of Ti-600 alloy extended to the aerospace and aircraft industries. Considering the practical application of the alloy, high cycle fatigue properties of the alloy must be investigated.

This paper presents and discusses the results of a recent study aimed at understanding the high cycle fatigue, resultant fracture behavior and intrinsic microstructural features of a near alpha (α) titanium alloy in the solutioned and aged condition. The high cycle fatigue response of the alloy was determined at two different load ratios ($R = \sigma_{min}/\sigma_{max}$) of 0.1, and −1 over a range of maximum stress and resultant cyclic fatigue life.

2. Experimental materials and procedures

A near-α high-temperature Ti-600 (Ti–6Al–2.8Sn–4Zr–0.5Mo–0.4Si–0.1Y) titanium alloy was used in this study. A 200 kg ingot was produced by electrode consumption vacuum arc furnace. The β transus temperature for the alloy is about

* Corresponding author at: Northwest Institute for Nonferrous Metal Research, Weiyang Road 96, Xi'an 710016, Shaanxi, PR China. Tel.: +86 29 86231078; fax: +86 29 86360416.
E-mail addresses: ZENG-ly@163.com, ZENG-ly@sohu.com (Z. Liying), trc@c-nin.com (Z. Yongqing).

0925-8388/$ – see front matter © 2010 Elsevier B.V. All rights reserved.
doi:10.1016/j.jallcom.2010.10.144

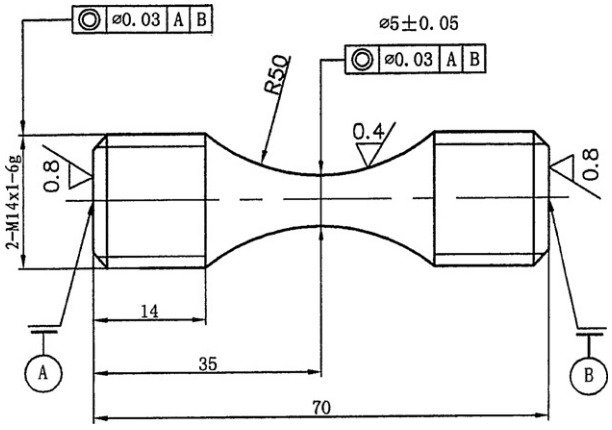

Fig. 1. Schematic figure for HCF specimens.

1010 °C. The alloy was forged at 1100 °C from a 240 mm starting diameter to a 90 mm square cross-section. Then diameter 32 mm bars were conventionally forged. The forging was eventually rolled to diameter 16 mm bars at temperatures below 950 °C. The relatively low temperature range for rolling was selected to obtain fine grains. The fatigue samples were cut from the rolling bars and were solutioned at 1020 °C for 1 h, air cooling, then aged at 650 °C for 8 h, air cooling (STA).

Tensile tests were conducted with smooth cylindrical specimens having a 5 mm diameter by 25 mm gauge length using an Instron-1185 electron tensile machine at a strain rate of 3.3×10^{-3} s^{-1}. Smooth axial fatigue tests were carried out on the fatigue specimens schematically shown in Fig. 1 of 5 mm gauge diameter using a QBG-100 high cycle fatigue tester at a frequency of 120–130 Hz with load ratios R of 0.1 and −1, respectively.

The samples for microstructural examination were cut from the specimens fatigued for different time fractions, mounted first in bakelite and then polished following standard metallographic practice. Subsequently the samples were etched using Kroll's reagent and were examined using Olympus PMG3 optical microscopy.

Fractographies after fatigue interrupted tests were performed on JSM 6460 scanning electron microscopy (SEM). Thin foils for TEM observations were prepared from longitudinal sections of fatigued specimens. They were mechanically thinned on papers with grades 600 and 1200 to a thickness of 60 μm, then electrolytically thinned to electron transparency with a solution composed of 6% perchloric acid, 20% butylglycol, and 70% methanol at −30 °C. Microstructures were observed on JEM 2010 transmission electron microscopy (TEM).

3. Results and discussions

3.1. Mechanical properties for Ti-600 alloy

Table 1 shows the tensile properties of Ti-600 alloy at ambient temperature and at 600 °C. From the table, it can be seen that after appropriate thermal treatment, the ultimate strength (UTS) for the alloy at ambient temperature is about 1000 MPa, the elongation (EL) is not less than 10%. While at 600 °C, the UTS and EL is higher than 660 MPa and 15%, respectively. The results above indicate that the alloy possesses favorite combination of strength and plasticity at ambient temperature and at 600 °C, also indicate that the alloy may be the potential candidate alloy which can be used at 600 °C.

Table 1
Mechanical properties of Ti-600 alloy bars solutioned at 1020 °C for 1 h, plus aged at 650 °C for 8 h, air cooling.

Testing temperature (°C)	UTS (MPa)	Y S (MPa)	E L (%)	R A (%)
20	1000	925	11.5	15.5
	995	915	15.0	17.0
600	665	540	15.0	32.5
	660	540	15.5	29.5

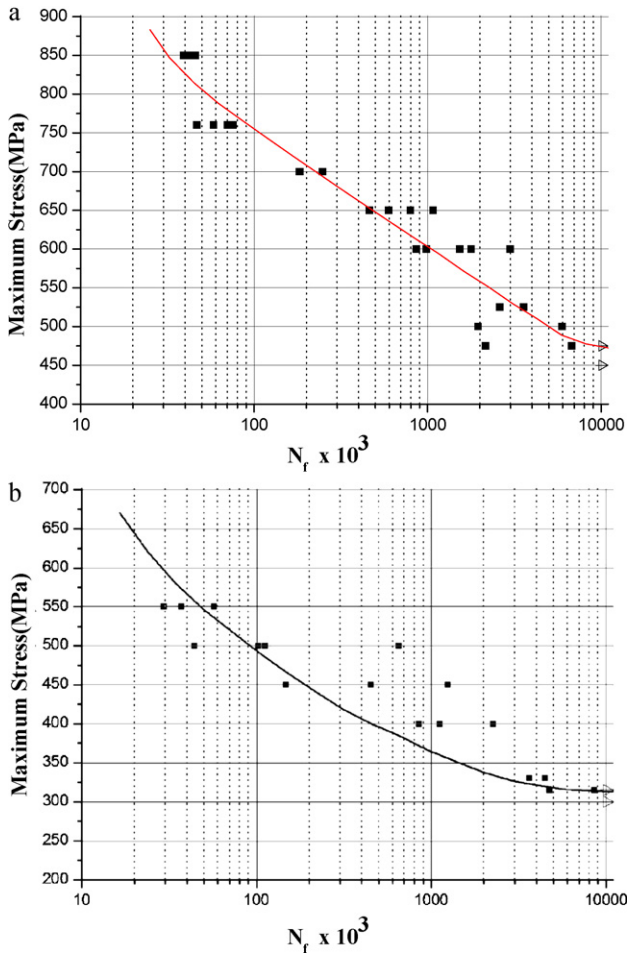

Fig. 2. Maximum stress as a function of number of cycles to failure for Ti-600 alloy at a load ratio of 0.1 (a) and at a load ratio of −1 (b), samples tested at ambient temperature.

3.2. HCF property of Ti-600 alloy at ambient temperature

Since fatigue damage is cumulative the occurrence of fracture depends on the magnitude and duration (number of cycles) of the individual cyclic loads which act on the structure throughout its life. Engineering fatigue data is normally represented by means of S–N curve, a plot of stress S against the number of cycle, N_f. The curves of maximum stress versus number of cycles to failure for Ti-600 alloy are shown in Fig. 2. In many industries, the required design lifetime of many components often exceeds 10^7 cycles. Present experimental results show the fatigue failures of the high-temperature titanium alloys (Ti-600) take place in the high cycle regime (10^7 fatigue cycles).

Table 2
Smooth axial fatigue strength of Ti-600 alloy and other two titanium alloys at ambient temperature cycled at 10^7 cycles.

Alloy	R	Fatigue strength (MPa)	Processing
Ti-1100	0.1	655[a]	β forged and annealed bar
IMI834	0	500 ± 25[a]	Cast, α + β HIP, plus 0.5 h at 1070 °C, OQ and plus 2 h at 700 °C
IMI834	0	500[a]	Wrought, 50 mm diameter bar
Ti-600	−1	315	α + β forged and STA
Ti-600	0.1	475	α + β forged and STA

[a] The HCF strengths for the titanium alloys listed in the table are from Ref. [10].

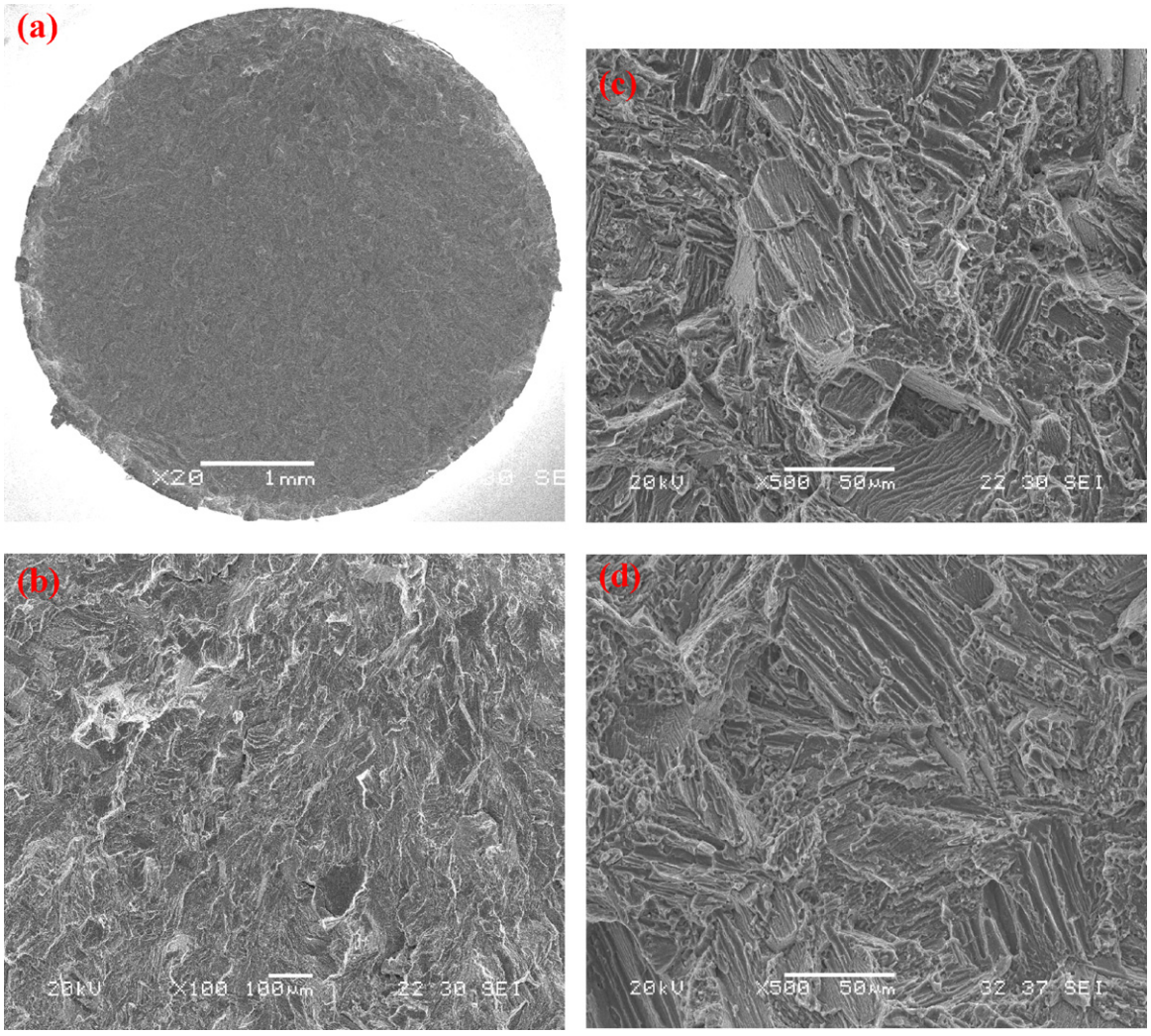

Fig. 3. Scanning electron micrograph of high cycle fatigue fracture surface of the Ti-600 alloy deformed at maximum cyclic stress of 600 MPa ($R = 0.1$), fatigue life $N_f = 1.78 \times 10^6$ cycles (a–c), fatigue life $N_f = 8.61 \times 10^5$ cycles (d) showing [orientation: longitudinal]: (a) overall morphology showing the region of crack initiation. (b) High magnification of (a) showing a population of fine microscopic cracks in the region of early crack growth. (c) Narrower striation-like features in the region of stable crack growth with fatigue life of 1.78×10^6 cycles, and the well-developed secondary cracks oriented nearly perpendicular to the main cracks. (d) Wider striation-like features in the region of stable crack growth with fatigue life of 8.61×10^5 cycles, and the secondary cracks locate at phase-boundaries or in the β-phase.

From the curve, it can be seen that the HCF strength at ambient temperature for the smooth specimens cycled at 10^7 cycles with the load ratio R of 0.1 and −1 is found to be 475 MPa, 315 MPa, respectively. Table 2 shows the smooth axial fatigue strength of Ti-600 alloy and other two titanium alloys (e.g. Ti-1100, IMI834) at ambient temperature. From the table, we can see that the HCF strength for the cast and wrought IMI834 alloy is 500 MPa or so [11]. Comparing the HCF strength after 10^7 cycles among the alloy and the other two high temperature titanium alloys, it can be concluded that the HCF strength of Ti-600 alloy with a load ratio R of 0.1 is comparable to that of IMI834 alloy.

3.3. Fractographies observation for Ti-600 alloy

At load ratio R of 0.1 and maximum stress of 850 MPa, the longitudinal smooth specimen had a fatigue life of 4.60×10^4 cycles. Fractographies for the alloy fatigue at 600 MPa with a fatigue life of 1.78×10^6 cycles and 8.61×10^5 cycles are shown in Fig. 3. At load ratio R of −1 and maximum stress of 550 MPa, the longitudinal smooth specimen had a fatigue life of 3.72×10^4 cycles. Fractographies for the alloy fatigue at 550 MPa with a fatigue life of 3.72×10^4 cycles are shown in Fig. 4. As shown in Figs. 3a and 4a, the fracture surfaces reveal that fatigue cracks are initiated at the surface of the specimens and the fracture surfaces include three typical fracture zones: (I) crack initiation area; (II) crack propagation area and (III) fast fracture area. In most Ti-600 alloy samples, only one nucleation site is found on the failure surface, other sites may have nucleated and do not propagate to failure.

3.3.1. Load ratio (R) = 0.1

Scanning electron microscopy observations shown in Fig. 3 reveal the overall morphology at low magnification to comprise a smooth, small yet distinct region of crack initiation and early microscopic crack growth, which occurring radially into the microstructure and away from the crack initiation site (Fig. 3a). Slip lines are formed during the first few thousand cycles of stress. Back and forth fine slip movements of fatigue could build up notches or ridges at the surface, which can initiate cracks. In this stage, the fatigue crack tends to propagate initially along slip planes and later take the direction normal to the maximum tensile stress. The crack propagation rate in this stage is generally very low on the order of nm/cycles. Higher magnification observation of this region reveals

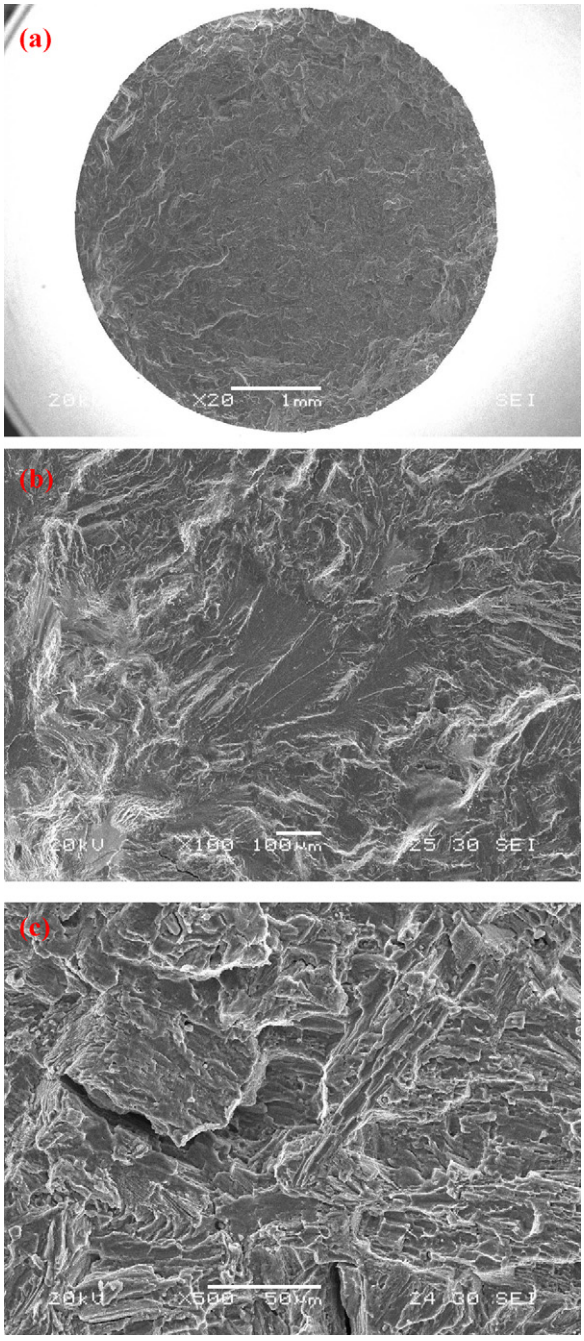

Fig. 4. Scanning electron micrograph of high cycle fatigue fracture surface of the Ti-600 alloy deformed at maximum cyclic stress of 550 MPa ($R = -1$), fatigue life $N_f = 3.72 \times 10^4$ cycles showing [orientation: longitudinal]: (a) overall morphology showing the region of crack initiation. (b) High magnification of (a) showing a population of fine microscopic cracks in the region of early crack growth. (c) Fine isolated microscopic cracks and shallow striation-like features in the region of stable crack growth.

a population of extremely very fine microscopic cracks that are randomly distributed (Fig. 3b).

At large stress amplitudes, a very large fraction of fatigue life is spent in the growth or propagation of a crack. Observation at the higher allowable magnifications of the SEM reveals that crack propagation frequently shows a pattern of ripples or fatigue striations in the region of stable crack growth (Fig. 3c). Each striation is produced by a single stress cycle and represents the successive position of an advancing crack front normal to the greatest tensile stress. The distance of striations is quite different for various samples or even at disparate places in a same sample. At the same condition, the expansion rate of cracks should be small for the samples with small striation distance; on the contrary, fatigue crack resistance should be small for the samples with large striation distance. With the same stress of 600 MPa, the striation distance for the sample with a fatigue life of 8.61×10^5 cycles is wider than that of the sample with a fatigue life of 1.78×10^6 cycles, which means, the fatigue crack resistance is smaller and the fatigue crack could expand easily for the former. One can also see that the striations become larger from the fatigue crack initiation site (Fig. 3b) to the crack propagation area (Fig. 3c) indicating an increase in fatigue crack propagation rate.

After large number of cycles to fracture, extensive secondary cracking at the center of the samples can be observed. The main fatigue cracks are transcrystalline for all samples, whereas the secondary cracks exhibit significant differences. The sample with a fatigue life of 8.61×10^5 cycles show secondary cracks locate at phase-boundaries or in the β-phase, while the sample with a fatigue life of 1.78×10^6 cycles show well-developed secondary cracks oriented nearly perpendicular to the main crack. This has a positive effect on the fatigue life [12].

A population of dimples of varying size and shape are found covering the region of overload (Fig. 3a).

3.3.2. Load ratio (R) = −1

The overall morphology of the fatigue fracture surface shown in Fig. 4 reveals the distinct regions of fatigue deformation and overload. As shown in Fig. 4a, the crack growth occurs radially into the microstructure and away from the crack initiation site. Observation of this region of the fatigue fracture surface at higher allowable magnifications reveals an array of macroscopic and fine microscopic cracks oriented parallel to the major stress axis (Fig. 4b). A healthy population of fine isolated microscopic cracks distributed through the transgranular region and shallow striations of localized micro-plastic deformation are evident in the region of stable crack growth at the higher magnifications of the scanning microscope, as shown in Fig. 4c.

3.4. Microstructures of Ti-600 alloy

In order to determine the relevant damage mechanisms during cyclic deformation of the Ti-600 alloy, a detailed microstructural characterization was performed using OM and TEM on the samples prior to and after fatigue testing.

3.4.1. Optical microstructures of Ti-600 alloy prior to and after fatigue tests

Fig. 5 shows the optical microstructures for Ti-600 alloy before and after fatigue tests. The alloy was solutioned at 1020 °C (β transus temperature is 1010 °C or so). When the solution treatment temperature increased to above the β transus temperature, evenly distributed transformed β microstructure can be found in the alloy, and the microstructure for the alloy is fine lamellar α plus β, as shown in Fig. 5a. Fig. 5 also shows the microstructure of the alloy fatigued with different load ratios. The morphologies of the alloy after fatigue tests are almost the same as that of the alloy before fatigue tests. The short primary α grains grow up, α plus β lamellar in transformed β grains elongate apparently, as shown in Fig. 5b for the alloy fatigued with a load ratio of 0.1, the elongated morphology has relation to a consequence of the rather high heat treatment temperature and large number of fatigue cycles (Fig. 5b). Obviously, coarsened and twisted transformed β grains can be found at the same time. However, only a slight grain coarsening can be found, as shown in Fig. 5c for the alloy fatigued with a load ratio of −1. From Ref. [13], it can be known that the overlapping plate like structure are benefit to prevent of the expansion fatigue cracks,

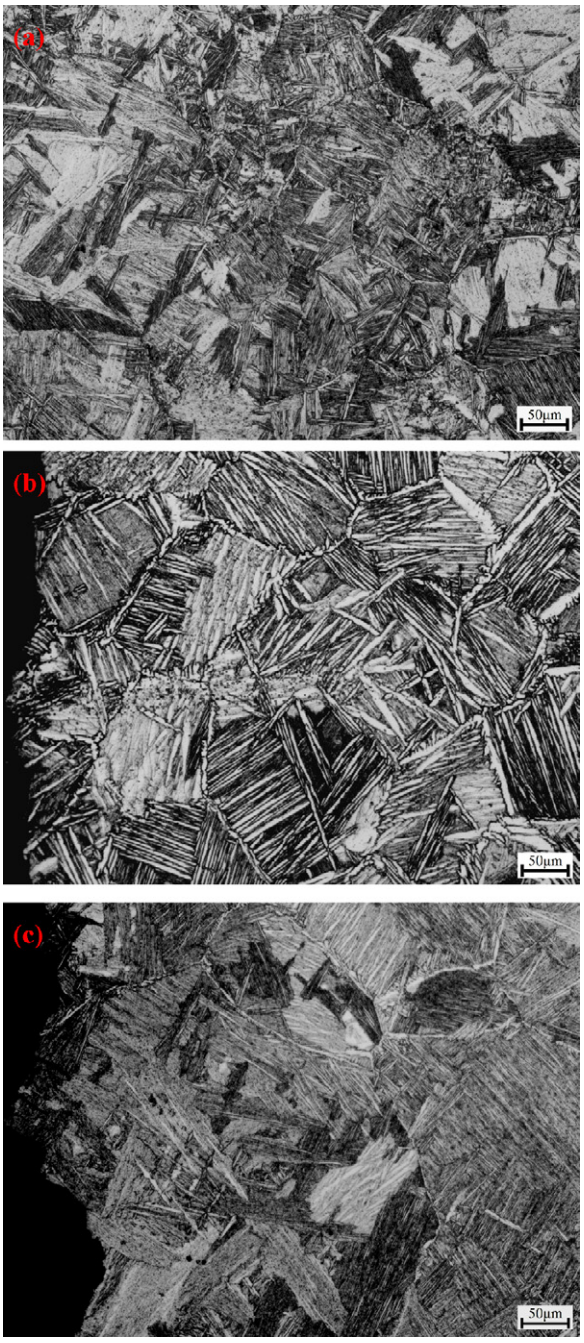

Fig. 5. Microstructures of Ti-600 alloy. (a) Before fatigue test; sample solutioned at 1020 °C for 1 h, then aged at 650 °C for 8 h, air cooling. (b) Sample fatigued at maximum cyclic stress of 760 MPa ($R = 0.1$), fatigue life $N_f = 7.02 \times 10^4$ cycles. (c) Sample fatigued at maximum cyclic stress of 550 MPa ($R = -1$), fatigue life $N_f = 3.72 \times 10^4$ cycles.

hence to improve the fatigue life for titanium alloy. More coarsened and twisted transformed β microstructures, better fatigue property. That is the reason why the alloy fatigued with a load ratio of 0.1 has a better fatigue strength.

3.4.2. Optical microstructures of Ti-600 alloy fatigued with different fatigue life

Fig. 6 shows the optical microstructures of Ti-600 alloy fatigued at maximum cyclic stress of 600 MPa with load ratio R of 0.1 with fatigue life of 1.7808×10^6 cycles (former) and 8.61×10^5 cycles (latter). The overlapping plate like structure (transformed β, fine lamellar α plus β) can be found in the figures. The morphology

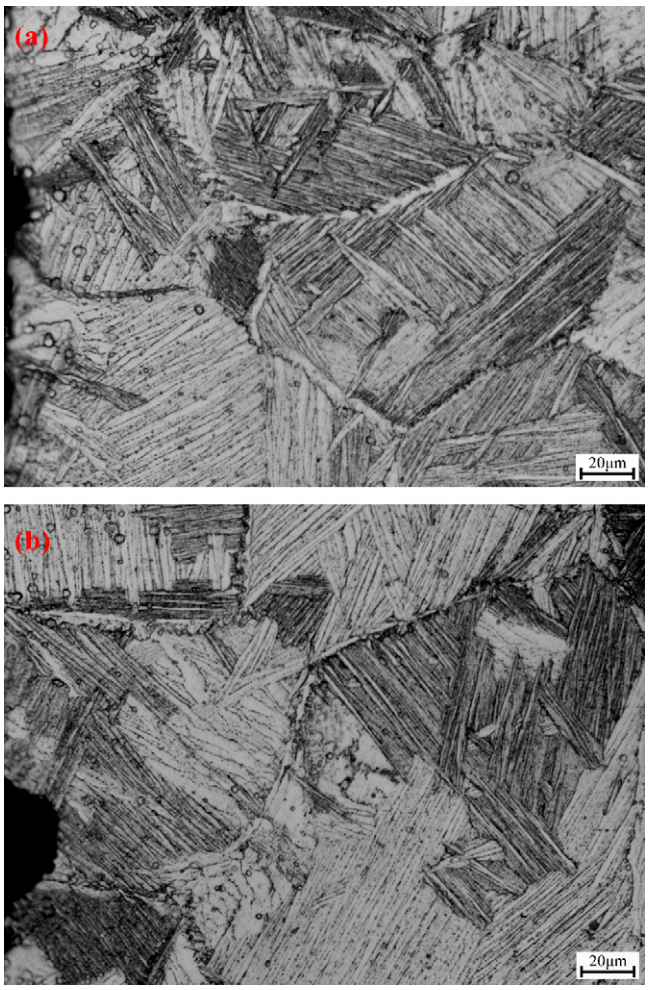

Fig. 6. Optical microstructures of Ti-600 alloy, samples fatigued at maximum cyclic stress of 600 MPa with a load ratio R of 0.1, fatigue life $N_f = 1.7808 \times 10^6$ (a); fatigue life $N_f = 8.61 \times 10^5$ (b).

of transformed β microstructure has a significant effect on the resistance ability of crack expansion, which mainly influences the crack propagation area. No significant differences exist in the alloy fatigued with two different kinds of fatigue lives. α lathes precipitated at grain boundaries for the former are wider and coarsened than the latter, and more α lathes can also be found at grain boundaries for the former. The interlacing transformed β microsructures for the former arrange heavily. That is the reason why the former has better fatigue life than the latter for the samples fatigued at the same stress.

3.4.3. Influence of elements Y, Mo and Zr to the microstructures of Ti-600 alloy

Fig. 7 shows the morphologies of rare earth (RE) particles (phases) in Ti-600 alloy after fatigue tests. Most of the RE particles in the alloy are ellipsoidal, some are sphere, some even are irregular shapes as polygonal, etc. The distribution of RE phases is unevenly, and the size of the RE phases varies from several micrometers to 0.2 μm. As shown above, cracks are originated from the sample surface or subsurface. Fatigue cracks would usually originate from bigger size rare earth phases mainly for localized stress concentration around RE phases, seldom from smaller size RE phases. Smaller size RE phases have some effect on the expansion of cracks. That is the reason why no crack initiation related to RE phase particles is found in Ti-600 alloy.

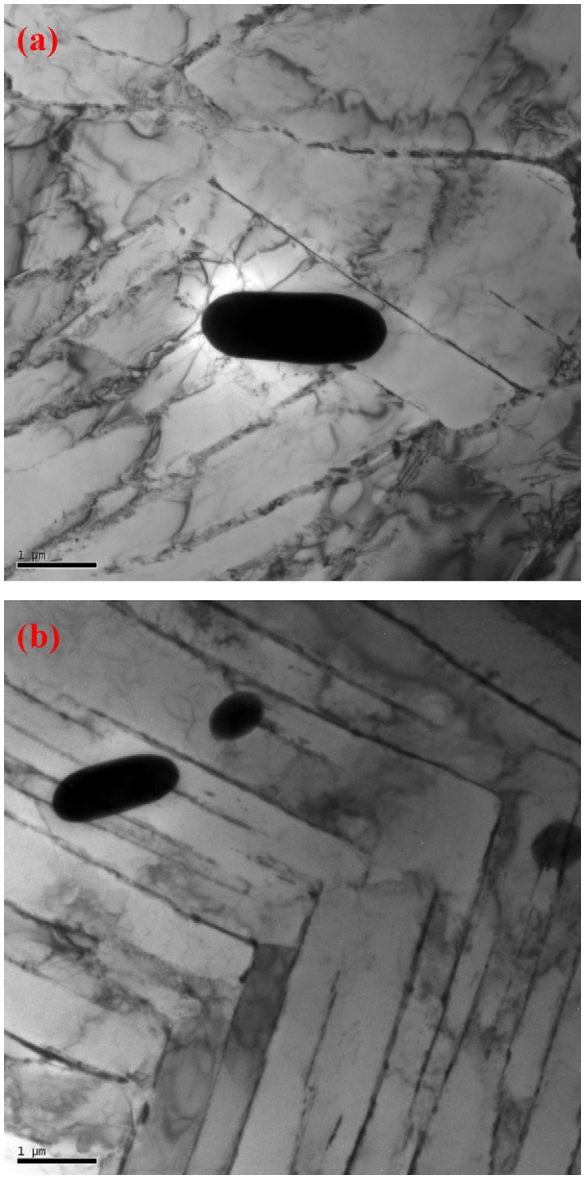

Fig. 7. Morphologies of rare earth particles in Ti-600 alloy, samples fatigued at the cyclic stress of 500 MPa ($R = 0.1$), fatigue life $N_f = 9.527 \times 10^5$ cycles. (a) Larger size particles; (b) intermediate and smaller size particles.

Due to previous hot rolling the microstructure is rather fine with a high dislocation density, however, after fatigue tests, decreased dislocation densities inside most grains are visible, as shown in Fig. 7. Due to cyclic deformation, a significant rearrangement of the initial dislocation structure leading to cyclic softening takes place. After that, the new microstructural arrangements become stable and lead to a pronounced saturation stage. Hence, it is supposed that the dislocation densities decrease and a small rearrangement of the dislocation structures take place during cyclic deformation. In all cases, the grain boundaries play a significant role in the annihilation of dislocations during cyclic deformation [14,15].

At the same time, elements Mo and Zr were added into Ti-600 alloy, which not only reinforce the alloy, but also make the grain size of the alloy smaller. As shown before, the microstructure for the solutioned and aged alloy consists of fine and thin plate-like $\alpha + \beta$ phase, which makes the alloy exhibit high tensile strength (as shown in Table 1, the UTS for the alloy is not less than 1000 MPa) and high HCF strength.

4. Conclusions

Smooth axial fatigue tests were taken at a frequency of 120–130 Hz and with load ratios R of 0.1 and −1 for solutioned plus aged Ti-600 alloy cycled at 10^7 cycles. The main conclusions can be drawn as follows:

1 The high cycle fatigue (HCF) strength at ambient temperature is found to be 475 MPa for the alloy fatigued with a load ratio R of 0.1, and which is 315 MPa with a load ratio R of −1.
2 At the same stress of 600 MPa, the sample with a fatigue life of 1.78×10^6 cycles has a better fatigue resistance than that of the sample with a fatigue life of 8.61×10^5 cycles, because of its smaller striation distance, its well-developed secondary cracks, more wider and coarsened α lathes precipitated at grain boundaries, and the heavily arranged interlacing transformed β microsructures.
3 Overlapping plate like $\alpha + \beta$ phase microstructures can be found for Ti-600 alloy, which has contribution to improve HCF strength and prolong its fatigue crack propagation life.
4 The average grain size of rare earth phases in Ti-600 alloy ranges from several micrometers to 0.2 μm, no cracks corresponding to rare earth particles can be initiated.

Acknowledgments

The authors wish to thank financial support both from the National Key Basic Research and Development Program of China (No. 2007CB613807) and National Key Technology R&D Program (2007 BAE07B01).

References

[1] G. Lütjering, Mater. Sci. Eng. A243 (1998) 32–45.
[2] R.R. Boyer, Mater. Sci. Eng. A213 (1996) 103–114.
[3] D. Eylon, S. Fujishiro, P.J. Postans, F.H. Froes, J. Met. 36 (1984) 55–62.
[4] H. Chandler, Heat Treaters's Guide: Practices and Procedures for Nonferrous Alloys, ASM International, Ohio, 1996.
[5] P.J. Bania, J. Met. 3 (1988) 20–22.
[6] I. Weiss, S.L. Semiatin, Mater. Sci. Eng. A263 (2) (1999) 243–256.
[7] L.Y. Zeng, Q. Hong, G.J. Yang, Y.Q. Zhao, Y.L. Qi, P. Guo, Trans. Nonferrous Met. Soc. China 17 (Special 1) (2007) s522–s525.
[8] Q. Hong, Z.Q. Zhang, G.J. Yang, G.Z. Luo, Acta Metall. Sin. 38 (Suppl.) (2002) 135–137 (in Chinese).
[9] W.F. Cui, C.M. Liu, L. Zhou, G.Z. Luo, Mater. Sci. Eng. A323 (1–2) (2002) 192–197.
[10] C.H. Tao, Q.Q. Liu, C.X. Cao, et al., Faliure and Prevention of Aeronautical Titanium Alloy, Defence Industrial Press, Beijing, 2002 (in Chinese).
[11] R. Boyer, G. Welsch, E.W. Collings, Materials Properties Handbook: Titanium Alloys, ASM International, Ohio, 1994.
[12] L.R. Saitova, H.W. Höppel, M. Göken, I.P. Semenova, R.Z. Valiev, Int. J. Fatigue 31 (2009) 322–331.
[13] L. Zeng, Y. Zhao, X. Mao, Y. Qi, Mater. Sci. Forum 546–549 (2007) 1535–1540.
[14] L. Kunz, P. Lukas, M. Sloboda, Mater. Sci. Eng. A424 (1–2) (2006) 97–104.
[15] A.Y. Vinogradov, V.V. Stolyarov, S. Hashimoto, R.Z. Valiev, Mater. Sci. Eng. A318 (2001) 163–173.